Crystal Structure and Solid-State Reactivity of a Cd(II) Polymeric Complex with Acetylenedicarboxylic Acid

Stavroula Skoulika,*,† Panagiotis Dallas,† Michael G. Siskos,†
Yiannis Deligiannakis,‡ and Adonis Michaelides*,†

Department of Chemistry, University of Ioannina, 45110 Ioannina, Greece, and Department of Environmental and Natural Resources Management, University of Ioannina, Pyllinis 9, 30100 Agrinio, Greece

Received July 21, 2003. Revised Manuscript Received September 23, 2003

The novel one-dimensional coordination polymer $[Cd(ADC)(H_2O)_3]\ H_2O$, where ADC^{2-} = acetylenedicarboxylate dianion, was synthesized and characterized by single-crystal X-ray diffraction. The titled compound crystallizes in the monoclinic system, $P2_1/n$, $a = 6.908(1)$ Å, $b = 7.946(1)$ Å, $c = 16.390(1)$ Å, $\beta = 100.21(1)°$, $V = 885.4(2)$ Å^3, and $Z = 4$. The structure is made up of metal−organic chains linked by hydrogen bonds to form channels along the *b* axis. The carbon−carbon triple bonds are in close proximity (3.27 Å) along the *a* axis. This induces, upon heating, polymerization with formation of conjugated polycarboxylic chains. Detailed EPR studies have been performed in order to understand the polymerization process.

Introduction

The construction of molecular-based crystalline solids using metal−ligand, and/or hydrogen bonds has become a very active research field[1]. Materials with various interesting crystal architectures exhibiting adsorption[2], catalytic[3], magnetic,[4] or luminesence[5] properties have been reported in the literature.

In the recent years we have been using Cd^{2+} with aliphatic and aromatic dicarboxylic[6,7] and aromatic tricarboxylic acids[8] to construct metal−ligand/hydrogen-bonded coordination solids. We showed that the cation is always complexed by two carboxylate groups in the chelating mode, while the remaining (two or three) coordination sites are occupied by water molecules. These structures are always associated with extensive hydrogen-bonded networks involving both coordinated and lattice water molecules and carboxylate oxygen atoms. In the particular case of cadmium adipate[6] the 1D metal−organic chains formed were further linked by H-bonds ($R_2^2(8)$ in the graph-set notation), along both the *b* and *c* crystallographic axes. The ligand−ligand distance along both directions was about 5.5 Å and apparently is essentially controlled by the H-bond geometry. We then wondered if the ligand−ligand distance may be further decreased within reaction distance (<4.20 Å), by employing unsaturated dicarboxylic acids. In this case "in situ" polymerization would be possible either by heating or by using ionizing radiation.[9]

The ligand chosen in this work is acetylenedicarboxylic acid (H_2ADC). Crystal structures of some complexes of ADC^{2-} have been published in the literature.[10] In this work we show that Cd^{2+} with H_2ADC forms metal−organic chains assembled into a reactive 3D microporous solid, via H-bonds. Polymerization of H_2ADC has been achieved in the past by employing solvents and catalysts.[11]

Experimental Section

Preparations. $[Cd(ADC)\ (H_2O)_3]\ H_2O$, **1**. Colorless transparent crystals were formed within a few days, at room temperature, by slow evaporation of an aqueous solution resulting from the mixing of equal volumes (10 cm^3) of $Cd(NO_3)_2$ 0.1 M and H_2ADC 0.1 M at pH 6. The composition was established by X-ray crystallography.

The same compound was prepared in powder form by mixing equal volumes (50 cm^3) of aqueous solutions of $Cd(NO_3)_2$ 0.5

* Authors to whom correspondence should be addressed via e-mail: vskoul@cc.uoi.gr.
† Department of Chemistry.
‡ Department of Environmental and Natural Resources Management.

(1) (a) Batten, S. R.; Robson, R. *Angew. Chem., Int. Ed.* **1998**, *37*, 1461. (b) Moulton, B.; Zaworotko, M. J. *Chem. Rev.* **2001**, *101*, 1629. (c) Yaghi, O. M.; Li, H.; Davis, C.; Richardson, D. Groy, T. L. *Acc. Chem. Res.* **1998**, *31*, 474. (d) Holman, K. T.; Pivovar, A. M.; Swift, J. A.; Ward, M. D. *Acc. Chem. Res.* **2001**, *34*, 107.

(2) (a) Aoyama, Y. In *Design of Organic Solids* Weber, E., Ed.; Topics in Current Chemistry No. 198; Springer: New York, 1998; pp 132−159. (b) Eddaoudi, M.; Li, H.;. Reineke, T.; Fehr, M.; Kelley, D.; Groy, T. L.; Yaghi, O. M. *Top. Catal.* **1999**, *9*, 105. (c) Kitagawa, S.; Kondo, M.; Seki, K. *Angew. Chem., Int. Ed.* **2000**, *39*, 2082.

(3) (a) Fujita, M.; Kwon, Y. J.; Washizu, S.; Ogura, K. *J. Am. Chem. Soc.* **1994,** *116*, 1151. (b) Seo, J. S.; Whang, D.; Lee, H.; Jun, S. I.; Oh, J.; Jeon, Y. J.; Kim, K. *Nature* **2000**, *404*, 982.

(4) Kahn, O. *Acc. Chem. Res.* **2000**, *33*, 647.

(5) (a) Reineke, T. M.; Eddaoudi, M.; Fehr, M.; Kelley, D.; Yaghi, O. M. *J. Am. Chem. Soc.* **1999**, *121*, 1651. (b) Ma, L.; Evans, O. R.; Foxman, B. M.; Lin, W. *Inorg. Chem.* **1999**, *38*, 5837.

(6) Bakalbassis, E. G.; Korabik, M.; Michaelides, A.; Mrozinski, J.; Raptopoulou, C.; Skoulika, S.; Terzis, A.; Tsaousis, D. *J. Chem. Soc., Dalton Trans.* **2001**, 850.

(7) Michaelides, A.; Tsaousis, D.; Skoulika, S.; Raptopoulou, C.; Terzis, A. *Acta Crystallogr. Section B* **1998**, *54*, 657.

(8) Dimos, A.; Michaelides, A.; Skoulika, S. *Chem. Mater.* **2000**, *12*, 3256.

(9) Foxman, B. M. In *Crystal Engineering*; Rogers, R. D., Zaworotko, M. J., Eds.; ACA Transactions: Buffalo, NY, Vol. 33, 1999.

(10) Hohn, F.; Pantenburg, I.; Ruschewitz, U. *Chem. Eur. J.* **2002**, *8*, 4536

(11) (a) Yamaguchi, I.; Osakada, K.; Yamamoto, T. *Inorg. Chim. Acta* **1994**, *220*, 35. Masuda, T.; Kawai, M.; Higashimura, T. *Polymer* **1982**, *23*, 744.

10.1021/cm034666e CCC: $25.00
Published on Web 10/25/2003

Table 1. Crystal and Structure Refinement Data for Compound 1

chemical formula	$[Cd(ADC)(H_2O)_3]\ H_2O$
formula weight	296.52
space group	*P*21/*n*
T (K)	293(2)
a, *b*, *c* (Å)	6.908(1), 7.946(1), 16.390(1)
β (deg)	100.21(1)
V (Å^3)/Z	885.42(18)/4
ρ_{cald} (gcm^{-3})	1.744
unique reflections	1562
R1 ($I > 2\sigma(I)$)	0.0282
wR2 ($I > 2\sigma(I)$)	0.0702
GOF	1.064

Table 2. Coordination and Hydrogen Bond Lengths (Å) for Compound 1

Cd−O(3)	2.264(2)	Cd−O(2w)	2.270(3)
Cd−O(1)	2.365(3)	Cd−O(2w)	2.307(3)
Cd−O(2)	2.468(3)	Cd−O(3w)	2.279(3)
Cd−O(4)	2.660(3)		
O(1w)−H···O(1)	2.664(5)	O(2w)−H···O(2)	2.716(5)
O(1w)−H···O(2w)	2.917(5)	O(2w)−H···O(4w)	2.720(5)
O(3w)−H···O(3)	2.709(5)	O(4w)−H···O(4)	2.736(5)
O(3w)−H···O(4w)	2.783(5)	O(4w)−H···O(3w)[a]	3.104(5)
		O(4w)−H···O(1w)[a]	3.102(5)

[a] Three-center hydrogen bond.

M and H_2ADC (pH 6) 0.5 M. The precipitate was washed with a minimum amount of water and left to dry in air. The experimental X-ray powder diffraction (XRPD) pattern was in good agreement with that simulated from the single-crystal data. Anal. Calcd (%): C, 16.20; H 2.75. Found (%): C, 15.27; H, 2.55.

$[Cd(ADC)(H_2O)_{2.3}]$, **2**. Prepared by heating a powder sample of **1** in a furnace at 90 °C for about 1 h. The solid obtained by this method is EPR active. Anal. Calcd (%): C, 18.07; H, 1.75. Found (%): C, 17.66; H, 1.39.

This compound was also prepared at room temperature by mixing equal volumes (50 cm^3) of aqueous solutions of $Cd(NO_3)_2$ 0.41 M and H_2ADC (pH 6.2) 0.41 M. The precipitate was washed with a minimum amount of water and left to dry in air. This solid has an XRPD pattern identical to that obtained by heating **1** at 90 °C, but is EPR inactive.

[Cd(ADC)]·*x*H2O, **3**. Prepared by heating a powder sample of **1** in a furnace at 160 °C overnight.

Physical Measurements. Simultaneous TG-DTA analysis was carried out in air, at a scan speed of 5 °C/min, on a NETZSCH STA 449C apparatus. FT-IR spectra were recorded on a Perkin-Elmer Spectrum GX FT-IR spectrophotometer using the KBr technique. X-ray powder diffraction (XRPD) data were collected on a Bruker D8 Advanced System diffractometer. Simulation of the XRPD patterns was carried out with the CARine software. The EPR spectra were recorded at X-band on a Varian 109 spectrometer at room temperature. UV−Vis spectra were obtained on a Jasco UV/Vis/NIR V570 spectrophotometer.

Single-Crystal Structure Analysis. Data were collected at room temperature using a Bruker P4 diffractometer with monochromatic Mo Ka radiation. Crystallographic data are given in Table 1. The data were corrected for Lorentz and polarization effects. The structure was solved by direct methods using SHELXS-86 as implemented in SHELXL-97 software. All non-hydrogen atoms were refined anisotropically. Bond lengths and hydrogen bonding are given in Table 2. Drawings were made using SCHAKAL-97 software.

Results and Discussion

Crystal Structure. The structure of **1** consists of metal−organic chains running almost parallel to the [120] direction (Figure 1). Each ADC^{2-} dianion acts in the bis-bidentate chelating mode and is essentially planar. The Cd^{2+} cations are 7-coordinated by four

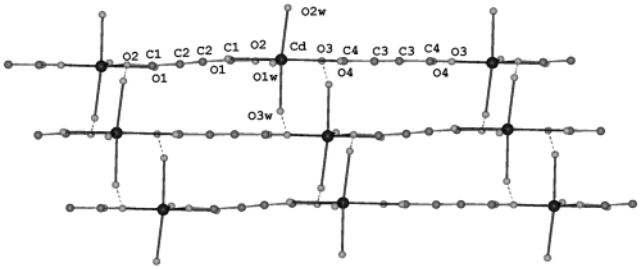

Figure 1. View of three chains forming a layer parallel to the *ab* plane. Dashed lines represent hydrogen bonds involving carboxylate oxygen−water and water−water interactions. The structure is further reinforced by numerous H-bonds linking the lattice water molecules (O4w) to the carboxylate oxygen atoms and the coordinated water molecules (Table 2).

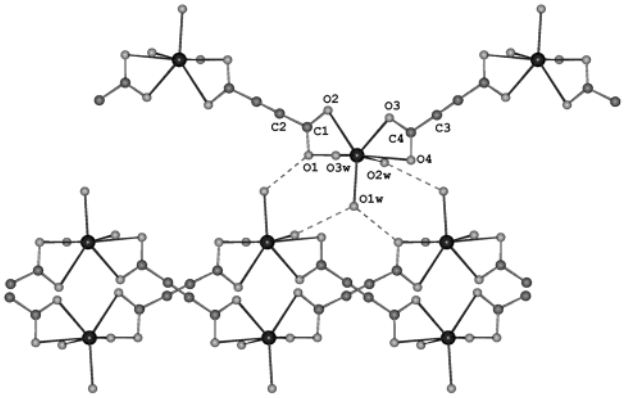

Figure 2. View of three chains forming a layer parallel to the *ab* plane. Dashed lines represent hydrogen bonds.

carboxylate oxygen atoms and three water molecules (Figure 2). Characteristic centrosymmetric ring-type (graph-set $R_2^2(8)$) hydrogen bonds connect the chains to form layers parallel to the *ab* plane (Figure 1). The H-links (Table 2) consist of complementary carboxylate oxygen−water interactions. The acetylene moieties of adjacent chains within a layer are parallel and rotated by 60° with respect to each other. Interestingly, the distance between the triple bonds is only 3.27 Å. Additional characteristic noncentrosymmetric ring-type H-bonds connect, along *c*, the chains belonging to neighboring layers (Figure 2). In this case the graph-set notation is also $R_2^2(8)$, but, the H-bonds involve carboxylate oxygen-water and water-water interactions. The structure is further reinforced by numerous H-bonds, linking the lattice water molecules (O4w) to the carboxylate oxygen atoms and the coordinated water molecules (Table 2). Relatively large channels filled with lattice water molecules are formed along *b* (Figure 3). The water structure is shown in Figure 4. The coordinated water molecules (O1w, O2w, O3w) and the lattice one (O4w) form pentagons propagating, through corner sharing, along the *b* axis. The water network involves a three-center (bifurcated) bond (Table 2). The sum of the three angles around the hydrogen atom that participates in this bond (351°), is close to 360°, satisfying well the criteria used for the existence of this type of bonding.[12] Edge-sharing water pentagons are formed in many protein and small molecule hydrates[12] but, as far

(12) Jeffrey, G. A. *An Introduction to Hydrogen Bonding*; Oxford University Press: New York, 1997.

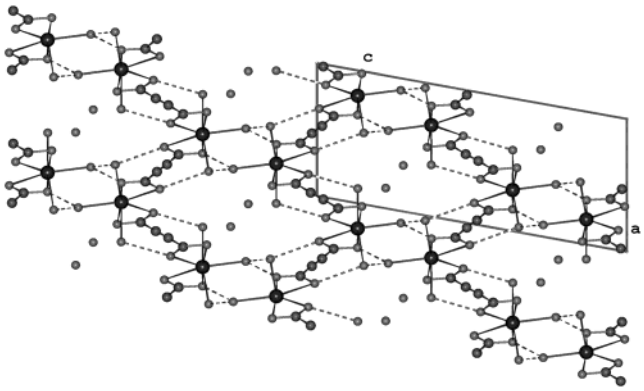

Figure 3. View of the structure along *b*, showing the channels filled with lattice water molecules.

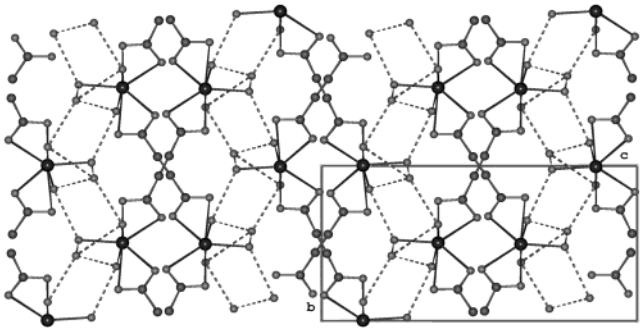

Figure 4. View of the structure along *a*. The corner-sharing pentagons formed by hydrogen-bonded water molecules are shown.

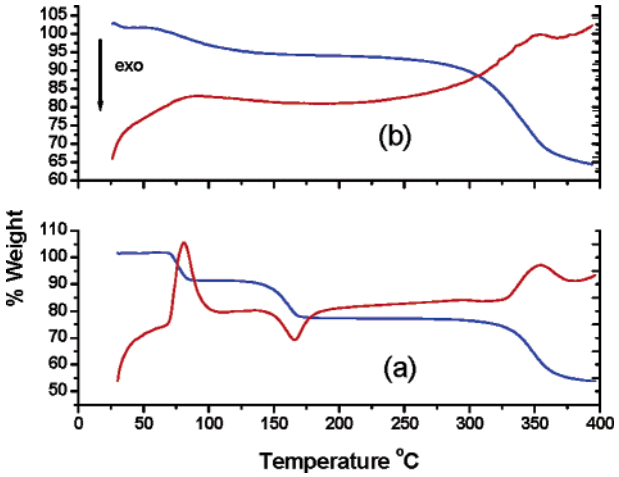

Figure 5. (a) TG (blue trace)/DTA (red trace) diagram of compound **1**. The second dehydration step, near 160 °C, is accompanied by the polymerization reaction resulting in a net slightly exothermic effect. (b) TG/DTA curves of compound **3**. The broad dehydration peaks indicate solvent "evaporation". The arrow indicates the direction of exothermic peaks.

as we know, this is the first time that corner-sharing pentagons are reported.

Thermal Analysis, Polymerization, and Phase Identification. Simultaneous TG-DTA experiments on compound **1** (Figure 5) showed that there is a first endothermic weight loss of 10.40% in the temperature range 70−90 °C, corresponding to the liberation of 1.7 mol of water per formula unit. The solid **2** obtained at the end of this step, is of very pale yellow color. A second weight loss of 14.26% corresponding to the liberation

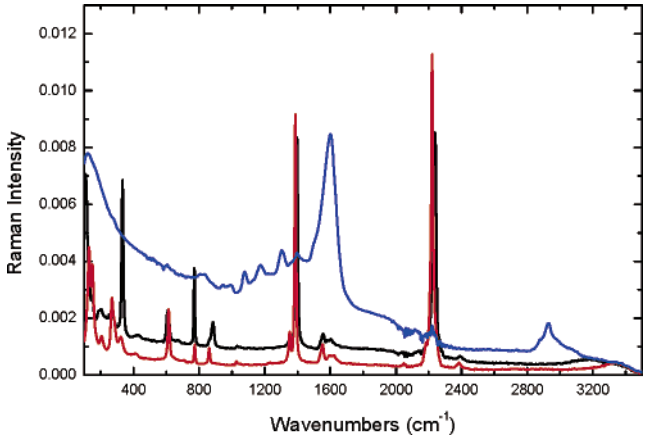

Figure 6. Raman spectra of compounds **1** (black trace), **2** (red trace), and **3** (blue trace).

of 2.3 mol of water per formula unit, occurs in the temperature range 140−170 °C, leaving a solid residue of yellow-brown color (**3**). Moreover, the latter transformation is slightly exothermic. The total weight loss (24.66%) is consistent with the liberation of all water molecules (calc. 24.29%). Compound **3** is stable up to 300 °C. Both dehydration steps are irreversible. The exothermic effect associated with the second dehydration step and the color of the completely dehydrated solid (**3**) suggest that the dehydration process is accompanied by other exothermic chemical reactions. The color, especially, was a strong indication that solid-state polymerization probably occurred. The Raman spectra fully confirm this interpretation (Figure 6). Compounds **1** and **2** exhibit very strong bands at 2239 and 2220 cm^{-1}, respectively, corresponding to the $\nu_{C\equiv C}$ vibration.[13] The quasi absence of this band in **3** shows that polymerization is almost complete.

Furthermore, this solid dissolved readily in a dilute aqueous nitric acid solution (approximately pH 1) and a viscous yellow solution was obtained. The electronic spectrum of an aqueous solution of **3** showed a maximum absorption at 203 nm which tails into the visible (up to approximately 600 nm, see Supporting Information). These features are compatible with the presence of a conjugated polycarboxylic polymer.[14] Dynamic light scattering measurements on an aqueous acidic solution confirmed this hypothesis, and the molecular weight found was 18 000 ± 2000 g/mol. The polymerization process was further studied by EPR spectroscopy (see below). We have already mentioned that there is close proximity (3.27 Å) of the triple bonds in **1** but thermal polymerization proceeds from the partially dehydrated compound **2**. The XRPD patterns (Figure 7) show that these two phases are not isostructural.

Attempts to solve the structure of **2** from powder diffraction data were not successful so far, but its space group ($P2_1/c$) is equivalent to that of **1** ($P2_1/n$). However, their vibration spectra (Figure 8), are strikingly similar. The large band in the region 3000−3500 cm^{-1} approximately in the IR spectra, denotes the presence of hydrogen-bonded water molecules in both complexes. In

(13) Long, D. A. *Raman Spectroscopy*; McGraw-Hill, New York, 1977.

(14) (a) Neoh, K. G.; Kang, E. T.; Tan, K. L. *Polymer* **1991**, *32*, 226. (b) Vosloo, H. C. M.; du Plessis, J. A. K. *Polymer Bull.* **1993**, *30*, 273.

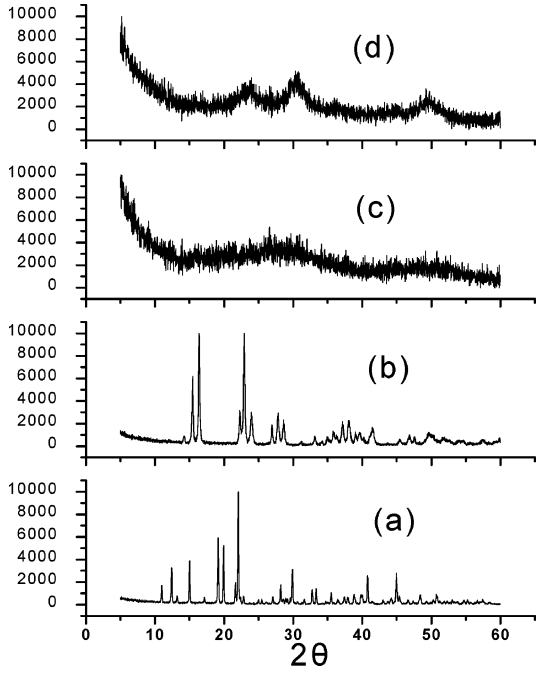

Figure 7. XRPD data of (a) compound **1**; (b) compound **2**; (c) anhydrous compound **3**; and (d) compound **3** reyhydrated.

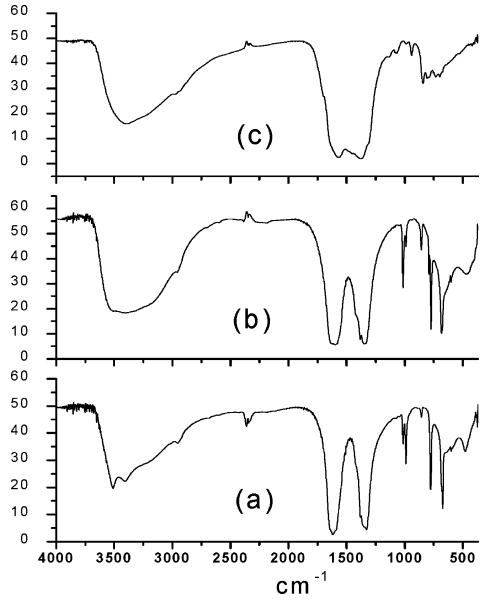

Figure 8. FT-IR spectra of compounds (a) **1**, (b) **2**, and (c) **3**.

the region of the stretching vibration of the carboxylate group (1700−1300 cm^{-1}), the splitting of ν_{sym} in **1** reflects well the nonequivalence of the carboxylate oxygen donor atoms[15] (see Table 2). We attribute this to the same reason as for the splitting of ν_{sym} or ν_{as} observed in compound **2**.

It is well-known that the difference Δ, between the asymmetric stretching vibration and the symmetric one ($\Delta = \nu_{as} - \nu_{sym}$), of the carboxylate group depends on its coordination mode.[16] We see that this difference is well above 200 cm^{-1} for **1** and **2** and may be correlated with "pseudo-unidentate" coordination due to significant differences in the Cd−O bond lengths for both carboxylate groups (see Table 2).[16] The value of Δ drops significantly after complete dehydration of **1** (compound **3**) and the two bands show considerable overlapping. These observations indicate profound changes in the coordination sphere of the metal. The low value of Δ, in this case, is compatible with the bridging, chelating-bridging, or "symmetric" chelating coordination modes of the carboxylate groups. The broadness of the two peaks suggests that all these modes are present. In addition, the presence of the alternant double bonds on the conjugate chains certainly contributes to the overlapping observed.[17] These trends are also obvious on the Raman spectrum of **3**. For compounds **1** and **2** we assign the weak doublet around 1600 cm^{-1} and the strong band around 1400 cm^{-1} (Figure 6), to the asymmetric (ν_{as}) and symmetric (ν_{sym}) stretching carboxylate vibrations, respectively. In compound **3** the difference $\nu_{as} - \nu_{sym}$ (Δ) decreases considerably. As a result, the two peaks overlap to give the large band around 1600 cm^{-1}. The $\nu_{C=C}$ of the conjugated chains appears also around 1600 cm^{-1} and certainly contributes to the enhancement and enlargement of this band.[17] The interpretation that naturally follows is that, upon complete dehydration of **2**, the hydrogen bonds holding the chains together (Figure 2) are replaced by stronger bridging carboxylate oxygen−metal bonds which link metals from two neighboring chains. This interpretation accounts well for the high thermal stability of this compound (Figure 5). In addition, on the Raman spectrum we may observe a weak band around 2950 cm^{-1} indicative of a C−H aliphatic bond. A possible and reasonable explanation is that this bond is the result of a dehydration/decarboxylation process which is very common in acrylic monomers and polymers. The decarboxylation process of carboxylic acid derivatives and dicarboxylic acids connected by single, double, and triple bonds has been extensively studied by Brill et al.[18] From these studies it was found that the water molecules play a crucial role, forming cyclic structures and facilitating the decarboxylation by reducing the energy barrier. Moreover, from kinetic studies it was found that the decarboxylation process is much slower than dehydration.[19] This accounts well for the thermal analysis results where only a mass loss due to dehydration was observed around 160 °C and for the elemental analysis of **3** that gave a lower percentage of C (16.5%) than expected (approximately 19%).[20]

If we make the reasonable assumption that compounds **1** and **2** have similar structures (similar vibrational spectra and same crystal symmetry) then compound **3** should possess channels comparable to those of **1** (Figure 3). Indeed, TG-DTA measurements carried out on a sample of **3**, left in contact with water overnight, showed a very broad endothermic peak in the range 25−150 °C (Figure 5), corresponding to about 1.5 mol of water per formula unit. This indicates that there

(15) Agterberg, F. P. W.; Kluit, H. A. J.; Dressen, W. L.; Oevering, H.; Buijs, W.; Lakin, M. T.; Spek, A. L.; Reedijk, J. *Inorg. Chem*. **1997**, *36*, 4321.

(16) Deacon, G. B.; Philips, R. J. *Coord. Chem. Rev.* **1980**, *33*, 227.

(17) Wojtkowcak, B.; Chabanel, M. *Spectrochimie Moleculaire, Technique et Documentation*, Technique et Documentation: Paris, 1977.

(18) (a)Belsky, J.; Maiella, P. G.; Brill, T. B. *J. Phys. Chem. A* **1999**, *103*, 4253. (b) Li, J.; Brill, T. B. *J. Phys. Chem. A* **2002**, *106*, 9491.

(19) (a) Eisenberg, A.; Yokoyama, T.; Sambalido, E. *Polym. Sci.: Part A1* **1969**, *7*, 1717. (b) Lattimer, P. R. *J. Anal. Appl. Pyrolisis* **2003**, *3*.

(20) For compound **3**, H%: Found = 1.31, Cald (for $x = 1.5$) = 1.20.

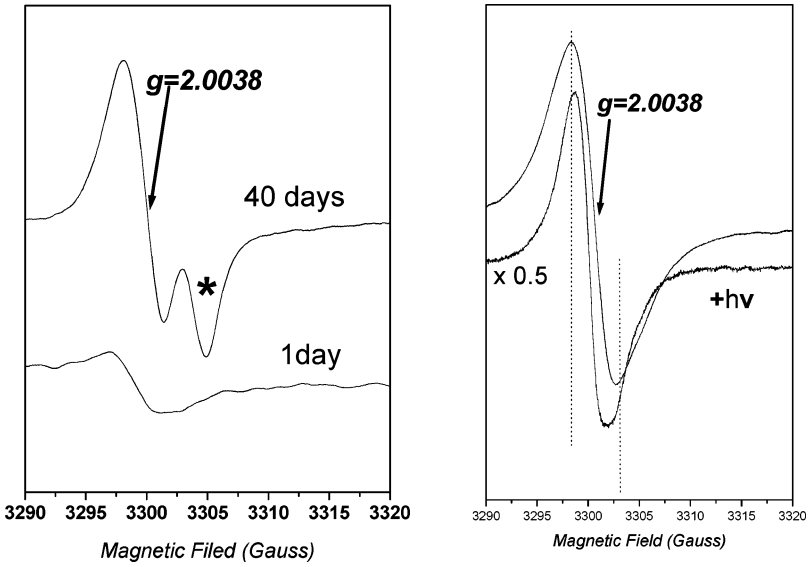

Figure 9. (left) EPR spectrum of compound **1** heated at 90 °C for different periods of time; and (right) EPR spectra of compound **1** heated at 160 °C for 24 h (upper trace), followed by subsequent X-ray irradiation for 6 h (lower trace).

is no phase transition during dehydration of **3** and that the process observed corresponds to solvent "evaporation".[21] The readsorption of water is accompanied by the appearance of some broad Bragg peaks in the XRPD pattern (Figure 7), indicating a drastic increase in crystallinity. We verified that the solvent is released reversibly. We therefore conclude that the porosity is permanent and not generated by the action of water on a nonporous solid.[22] However, we observe a nonporous behavior toward N_2 (surface area about 30 m^2/g), probably, because the kinetic diameter of N_2 (3.64 Å) is significantly greater than that of water (2.60 Å).[23]

Electron Paramagnetic Resonance Spectroscopy. To get more information about the polymerization process, we employed EPR spectroscopy which is very efficient in characterizing conjugated polymers. According to the thermal analysis results, compound **1** undergoes, upon heating, structural changes accompanied by color change. The characteristic temperature thresholds where these changes are observed are near 90 °C and 160 °C. Therefore, we have studied in some detail the EPR characteristics of the material at these temperatures. Compound **1** does not exhibit any EPR spectrum. Moreover, we observed that the color of the specimens changes upon X-ray irradiation. For this reason, we examined also the EPR spectra of compounds **1**, **2**, and **3** after X-ray irradiation. All EPR spectra are recorded at 300 K, microwave frequency of 9.265 GHz, modulation amplitude of 1.2 G, microwave power 1 mW, and modulation frequency 100 kHz. Spin quantitation was performed by comparing the double integral of the EPR signal of the sample with the EPR signal of a DPPH standard, both recorded under identical nonsaturating conditions. Within experimental error, it was found that the maximum radical concentration in the samples studied was 80% relative to that of the reference sample.

Thermal Treatment. Heating of compound **1** at 90 °C leads to the formation of paramagnetic centers. Representative EPR spectra are displayed in Figure 9. At short heating periods the radical centers are formed at low concentration, but at prolonged heating a significant amount of stable radicals is formed (Figure 9). The sample heated for 40 days is characterized by two radical signals. The main signal ($g = 2.0038$, $\Delta Hpp =$ 4.2 G) and a second one ($g = 2.0024$, $\Delta Hpp = 2.3$ G), marked by an asterisk in Figure 9, whose intensity depends linearly on the heating period length, corresponds, probably, to an isolated electron i.e., a localized defect.

The g value of the main signal is higher than that for a purely carbon-based radical.[24,25] Further analysis of the main radical by numerical simulation shows that this signal is Lorentzian and that it is homogeneously broadened.[26] Therefore, the T_2 of the radical can be calculated from the line width[26]

$$T_2 = \frac{10^{-6}}{7.6156 g \Delta Hpp} \text{ sec} \qquad (1)$$

which for $\Delta Hpp = 4.2$ G gives $T_2 = 156$ ns. Extended literature data in hydrocarbon polymers provide precedence for this type of EPR signals[25] as, for example, the case of radicals on long polyenes,[27] or allyl radicals.[25] In the case of compound **1**, the g value of the radical indicates that the electron is delocalized not only on carbons but to some extent on the carboxylate oxygens. The power saturation of this radical, $P_{1/2}$ (A) = 5.6 mW, is higher than that expected for an isolated radical in the solid state with restricted mobility.[25,26] Similar EPR characteristics have been previously reported for the

(21) (a) Gardner, G. B.; Kiang, Y.-H.; Lee, S.; Asgaonkar, A.; Venkataraman, D. *J. Am. Chem. Soc.* **1996**, *118*, 6946. (b) Jung, O.-S.; Park, S. H.; Kim, K. M.; Jang, H. G. *Inorg. Chem.* **1998**, *37*, 5781.

(22) Kiritsis, V.; Michaelides, A.; Skoulika, S.; Gohlen, S.; Ouahab, L. *Inorg. Chem.* **1998**, *37*, 3407.

(23) Reineke, T. M.; Eddaoudi, M.; Fehr, M.; Kelley, D.; Yaghi, O. M. *J. Am. Chem. Soc.* **1999**, *121*, 1651.

(24) Pshezhetskii, S. Ya.; Kotov, A. G.; Milinchunk, V. K.; Roginskii, V. A.; Tupikov, V. I. *EPR of Free Radicals In Radiation Chemistry*; J. Wiley & Sons: New York, 1974.

(25) Ranby, B.; Rabek, J. F. *ESR Spectroscopy in Polymer Research;* Springer-Verlag: Berlin, 1977.

(26) Poole, C. P. *Electron Spin Resonance*; Interscience Publishers Inc.: New York, 1967; p 705.

(27) Hanna, M. W.; McLachlan, A. D.; Dearman, H.; McConnel, H. M. *J. Chem. Phys.***1962**, *37*, 361.

Table 3. EPR Signals and Their Structural Assignments in Compound 1 after Heating and/or X-ray Irradiation

EPR signals	interpretation
X-ray irradiation	
singlet $g = 2.0038$ $\Delta Hpp = 4.4$ G	radical delocalized over carbons and oxygens
doublet $g = 2.0038$ $\Delta Hpp = 8.5$ G	weakly interacting radical pairs
Heating at 90 °C (compound **2**)	
singlet $g = 2.0038$, $\Delta Hpp = 4.2$ G	radical delocalized over carbons and oxygens
singlet $g = 2.0026$ $\Delta Hpp = 2.4$ G	secondary radical, defect
Heating at 90 °C + X-ray irradiation	
Interacting $S = 1/2$ pairs, $g = 2.0037$,	strongly interacting localized radical pairs $R < 12.4$Å
$S = 1/2$ $g = 2.0037$ radical interacting with two equivalent $I = 1/2$ protons, A = 62 G.	radical interacting with two equivalent H_2O protons.
$S = 1/2$ interacting with two inequivalent $I = 1/2$ protons, $A = 23$ G and $A = 12$ G.	radical interacting with two inequivalent protons.
Heating at 160 °C (compound **3**)	
singlet $g = 2.0038$ $\Delta Hpp = 4.4$ G	radical delocalized over carbons and oxygens
Heating at 160 °C + X-ray irradiation	
singlet $g = 2.0038$ $\Delta Hpp = 2.4$ G	exchange narrowing and relaxation enhancment; radical delocalized in the polymeric structure.

case of long polyene radicals of the type

$$[CH_2(CH{=}CH)_{m-1}CH{=}CH_2]^{\bullet} \quad m = 1, 2, 3, ...$$

where the unpaired electron is distributed over the $2m + 2$ carbon atoms in an alternant way.[27]

By heating compound **1** at 160 °C (compound **3**), irrespective of the heating period, only one kind of radical is observed. Representative EPR spectra are displayed in Figure 9. The spectrum is characterized by a single EPR derivative with g value 2.0038 and a line width of $\Delta Hpp = 4.4$ G. This radical is similar to the main one detected after heating at 90 °C, but posesses a higher radical concentration by a factor of 4−5.

Effect of X-ray Irradiaton. X-ray irradiation of compound **1** induces the formation of stable paramagnetic centers (Figure 10). The EPR spectrum consists of two types of overlapping spectra. One is a singlet ($\Delta Hpp = 4.5$ G, $g = 2.0037$), similar to that detected in the nonirradiated compounds **2** and **3**, due to a radical delocalized over carbons and oxygens, and one doublet ($g = 2.0037$, $\Delta Hpp = 8.5$ G), due to weakly interacting radical pairs.

$$\boldsymbol{H} = \beta\, \mathbf{B}\, \mathbf{g}\, \mathbf{S} + D\,[S_z^2 - S(S+1)/3] + E(S_x^2 - S_y^2) + \mathbf{S}\, \mathbf{A}\, \mathbf{I} \quad (2)$$

The simulated spectra have been generated for a total electron spin $S = 1$ and isotropic g tensors with $g = 2.0037$. The dipolar interaction is described by the terms D and E. According to the simulation, E is equal to zero which indicates an axial interaction between the two $S = {}^1/_2$ spins. The parameter D is determined by the distance R between the interacting radicals. If we assume that the interacting radicals are localized, i.e., in the so-called "point-dipole approximation", then D is given by

$$D = \frac{3g^2\beta^2}{2R^2} \quad (3)$$

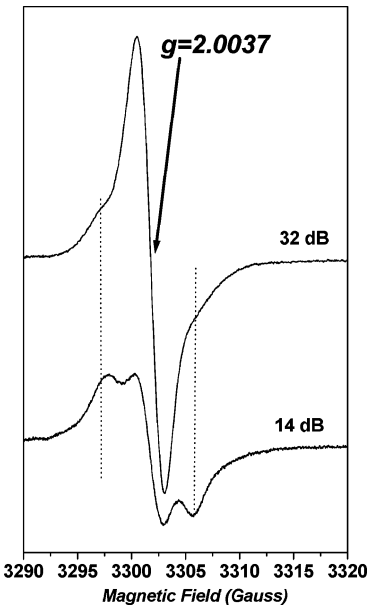

Figure 10. EPR spectra of compound **1** irradiated with X-rays for 6 h. The EPR spectrum of compound **2** changes dramatically upon irradiation, and becomes complex. It consists of three subspectra (i, ii, and iii in Figure 11), distinguished by their spectral shape and saturation properties. The different contributions can be distinguished by the aid of numerical simulations (Figure 11). Simulation of the spectrum has been performed by using the Spin-Hamiltonian (2).

Thus the estimation of D from the simulation of the EPR spectrum allows an estimation of the distance between the interacting radicals. According to this approach, $R = 12.6$ Å. This estimate is an upper limit of the distance if the radicals are delocalized. The term **S A I** in eq 2 is the hyperfine electron−nuclear coupling. In the simulation we have used two $\mathbf{I} = {}^1/_2$ nuclei with isotropic $\mathbf{A} = 21$ G. The parameters used for the simulation and the resulting interpretation of the subspectra are summarized in Table 3. We may assign the observed $\mathbf{I} = {}^1/_2$ hyperfine interactions, i.e., subspectra (ii) and (iii) in Figure 11, to the protons of the coordinated water molecules present in the structure.

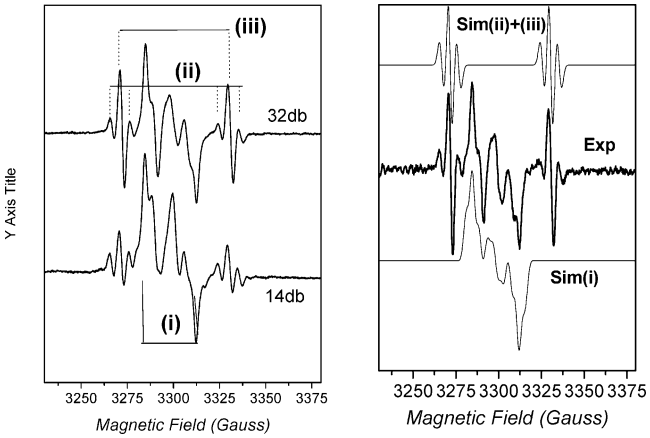

Figure 11. Experimental (left) and simulated (right) EPR spectra of compound **2** irradiated with X-rays for 6 h. The marks indicate the three types of EPR signals (i), (ii), and (iii), which contribute to the observed spectrum.

X-ray irradiation of **3** induces a narrowing in the EPR spectrum (Figure 9), with a concomitant increase in the signal intensity approximately by a factor of 2. The effect of irradiation on this compound is in striking contrast with the effect of irradiation on compound **2**. This observation is intriguing and its interpretation is not straightforward. In the following we attempt an explanation of the observed spectra in correlation with the structural properties of the compound. It is known from the thermal analysis that, at this temperature, no water molecules are present in the solid. Moreover, polymerization takes place in a large extent. The interchain connections that are formed by polymerization provide a covalent path which allows strong exchange interaction between the radicals. This leads to the observed narrowing of the EPR spectrum (Figure 9), accompanied by a strong relaxation as predicted by theory.[26,28]

Comments and Conclusions. The structure of compound **1** is the only known structure of acetylenedicarboxylato salts and complexes presenting short acetylene−acetylene contacts. The geometry and the distribution of ligands in the coordination sphere of the metal is crucial in bringing the chains within reactive distance (<4.2 Å). The Cd^{2+} cation proved to be effective to achieve this goal via formation of ring type $R_2^2(8)$ complementary hydrogen bonds between adjacent metal−organic chains. The engineering of preorganized solids presenting short acetylene−acetylene contacts, through formation of metal complexes of propynoic acid, has been discussed by Foxman.[9] He showed that this class of solids can undergo solid-state polymerization, by heating or by γ-irradiation, provided that they contain infinite chains of short acetylene−acetylene contacts.

The EPR data show that either thermal treatment or X-ray irradiation of compound **1** can create long-lived paramagnetic radicals. In all cases the main component is a radical with g near 2.0038 and a line width near 4.5 G. Its characteristics, i.e., *g* value, line shape, and relaxation properties, can be accounted for if we consider that it is delocalized over a chain fragment which involves alternant carbon bonds and the side carboxylates. From this result we may suppose that in all these samples a certain degree of polymerization has been accomplished. In compound **3** this process is practically complete. It is worth mentioning that the observed paramagnetic centers are remarkably stable. The intensities of the EPR signals of compounds **2** and **3** are within 5% unaltered after a period of more than one year.

The thermal behavior of **1** is also different from that observed in other complexes of H_2ADC.[10,29] Indeed, we previously mentioned that the partially dehydrated solid **2** contains already stable radicals. Moreover, the solid-state polymerization process at 160 °C is only slightly exothermic and overcomes the drawback of the large exothermic effect which usually accompanies the solid-state polymerization reactions.[30] We also verified that polymerization of **1** may be induced by γ-irradiation. A detailed study of the products obtained (nature of products, molecular weight, etc.) will be presented in a forthcoming article.

Acknowledgment. We thank Dr. T. Bakas for recording the XRPD spectra, Dr. T. Vaimakis for the thermal analysis measurements, Dr. J. Plakatouras for recording the FT-IR spectra, Dr. E. Kamitsos for assistance with the Raman spectroscopy, Dr. S. Hadjikakou for recording the UV-VIS spectra, and the Microanalytical Laboratory of the Chemistry Department of the University of Ioannina for the elemental analyses. We also thank the Authorities of the Region of Epirus for the purchase of the X-ray equipment.

Supporting Information Available: Tables of crystal data, structure solution and refinement, atomic coordinates bond lengths and angles, and anisotropic thermal parameters for **1** (cif) and the absorption spectra of **3** (pdf). This material is available free of charge via the Internet at http://pubs.acs.org.

CM034666E

(28) Longuet-Higgins, H. C.; Salem, L. *Proc. R. Soc. (London)* **1959**, *A251*, 172.

(29) (a) Allan, J. R.; Beaumont, P. C.; Macindoe, L.; Milburn, G. H. W.; Werninck, A. *Thermochim. Acta* **1987**, *117*, 51. Zamiduo, W.; Baraona, R. *Bol. Soc. Chil. Quim.* **1994**, *39*, 339.

(30) Herzberg, O.; Epple, M. *Eur. J. Inorg. Chem.* **2001**, 1395.